Subwavelength diffraction-free beams in metallic wire media

Juan J. Miret,[a] Carlos J. Zapata-Rodríguez,[b] Slobodan Vuković[c] and David Pastor[b]

[a]Department of Optics, Pharmacology and Anatomy, University of Alicante, P.O. Box 99, Alicante, Spain;
[b]Department of Optics, University of Valencia, Dr. Moliner 50, 46100 Burjassot, Spain;
[c]Center of Microelectronic Technologies and Single Crystals, Institute of Chemistry, Technology and Metallurgy, University of Belgrade, Njegoševa 12, 11000 Belgrade, Serbia

ABSTRACT

We present recent progress in nondiffracting subwavelength fields propagating in complex plasmonic nanostructures. In particular, diffraction-free localized solutions of Maxwell's equations in a periodic wire medium are discussed thoroughly. The Maxwell-Garnett model is used to provide analytical expressions of the electromagnetic fields for Bessel beams directed along the cylinders axes. Large filling factors of the metallic composite induce resonant-plasmonic spots with a size that remains far below the limit of diffraction. Some numerical simulations based on the finite-element method support our analytical approach.

Keywords: hybrid surface waves, superlattices, plasmonics

1. INTRODUCTION

Bessel beams are wavefields traveling in free space that are characterized by a prescribed propagation constant along a given direction and concurrently their transverse patterns are clearly localized.[1] Since intensity is confined around a characteristic axis despite of diffraction effects, soon they were coined diffraction-free beams. However, the Bessel beamsize is unambiguously limited by diffraction inasmuch as its FWHM is greater than half the wavelength.

Transferring such ideas to optically structured media is strikingly easy to do but still barely unexplored.[2] Head attention has been addressed to guided modes for long due to its key role in telecommunications systems. Since a host medium cannot route a wavefield by definition, confined nondiffracting beams may be interpreted as a tight focusing within bulk inhomogeneous media. Potential applications include femtosecond laser submicrochannel machining and optical trapping and guiding of micro- and nano-size objects.

Not long since we theoretically confirmed that a metal-dielectric stratified medium may sustain diffraction-free localized beams, even including losses in the materials.[3,4] In particular, the existence of Bessel plasmons deserves special attention.[5] We confirmed that grazing propagation is not sustained by canalization[6] but depends on the waveform itself. Additionally, the assistance of surface plasmons polaritons (SPPs) leads to subwavelength beamsizes.

Here we present recent progress of our research group in nondiffracting subwavelength fields circulating in complex plasmonic nanostructures. In particular, localized diffraction-free SPPs in a metallic wire medium are discussed thoroughly.

2. BESSEL BEAMS IN EFFECTIVE MEDIA

Let us first consider metallic wires of radius r, made of a bulk metal with permittivity ϵ_m. We assume a periodic squared distribution of this sort of wires in a way that a stands for the lattice period, as shown in Fig. 1. Note that $a \geq 2r$. Finally, the host medium has a dielectric constant ϵ_d. Also we assume that monochromatic

Further author information: (Send correspondence to C.J.Z.-R.)
C.J.Z.-R.: E-mail: carlos.zapata@uv.es, Telephone: +34 963543805

Metamaterials VII, edited by Allan D. Boardman, Nigel P. Johnson, Richard W. Ziolkowski, Proc. of SPIE
Vol. 8423, 84230V · © 2012 SPIE · CCC code: 0277-786X/12/$18 · doi: 10.1117/12.922122

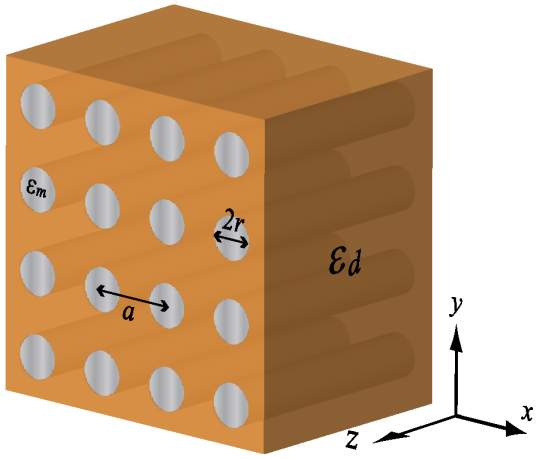

Figure 1. Periodic array of nanowires made of a metal with dielectric constant ϵ_m, distributed in a squared lattice, and hosted in a dielectric medium with permittivity ϵ_d. The radius of the wires is r and the lattice constant is a. Beam propagation is driven along the wires axes, that is the z axis.

beam propagation is driven along the wires, that is the z axis. If, additionally, the transverse waveform does not change at different xy planes, except maybe by a phase-only term depending on z, we may impose simultaneously that $\partial_z \mathbf{H} = i\beta\mathbf{H}$ and $\partial_t \mathbf{H} = -i\omega\mathbf{H}$, where $\omega = ck_0$ is the time-domain frequency and β is the on-axis spatial frequency of the wavefield. For convenience, the 3D magnetic field is written as $\mathbf{H} = \mathbf{H}_t + H_z\mathbf{z}$, where $\mathbf{H}_t$ includes both transverse components and H_z consider the on-axis component. Under these conditions, H_z satisfies the following wave equation,

$$\left(\epsilon k_0^2 - \beta^2 + \nabla_t^2\right) H_z = \epsilon \left(\nabla_t \epsilon^{-1}\right) \cdot \left(i\beta\mathbf{H}_t - \nabla_t H_z\right). \tag{1}$$

Here $\nabla_t = \mathbf{x}\partial_x + \mathbf{y}\partial_y$ and $\nabla_t^2 = \partial_x^2 + \partial_y^2$. In our system, a given wire axis is parallel to the unit vector $\mathbf{z}$; therefore we set $\epsilon(x, y) = \epsilon_m$ in the metallic rods and $\epsilon(x, y) = \epsilon_d$ in the host medium. As a consequence, nondiffracting solutions of the wave equation (1) includes hybrid solutions.

We may simplify our problem by considering the effective medium approximation (EMA). Under this approach, the structured medium is modeled as an anisotropic material. The EMA gives accurate results provided that the wavelength $\lambda_0 = 2\pi/k_0$ is significantly greater than the lattice period, $\lambda_0 \gg a$. As a consequence, $\epsilon(x, y)$ in Eq. (1) is transformed into an average constant parameter, $\epsilon_\perp$, which is given by

$$\epsilon_\perp = \epsilon_d \left[\frac{(1+f)\epsilon_m + (1-f)\epsilon_d}{(1-f)\epsilon_m + (1+f)\epsilon_d}\right], \tag{2}$$

where the filling factor $f = \pi r^2/a^2$. Here we use the expression for $\epsilon_\perp$ from the Maxwell-Garnett theory.[7] Moreover, Eq. (1) is reduced to a 2D Helmholtz equation, $\left(k_t^2 + \nabla_t^2\right) H_z = 0$, where $k_t = \sqrt{\epsilon_\perp k_0^2 - \beta^2}$ provided that $\epsilon_\perp > 0$ and $\beta < \sqrt{\epsilon_\perp} k_0$. This is a wave equation corresponding to nondiffracting ordinary waves propagating in a uniaxial crystal of permittivity $\bar{\epsilon} = \epsilon_\perp(\mathbf{xx} + \mathbf{yy}) + \epsilon_{||}\mathbf{zz}$. Solutions using Bessel functions come out naturally by setting ∇_t^2 in a cylindrical coordinate system, that is, $\nabla_t^2 = r^2\partial_r^2 + r\partial_r + \partial_\phi$. Solving the Helmholtz wave equation yields

$$H_z^o = \exp\left(i\beta z - i\omega t\right) \frac{k_t}{\beta} \sum_{m=-\infty}^{\infty} A_m \psi_m(r, \phi), \tag{3}$$

where A_m denotes a complex-valued constant, $\psi_m = \exp(im\phi) J_m(k_t r)$ and J_m is a Bessel function of the first kind. Equation (3) gives a complete solution provided that H_z^o does no diverge at $r = 0$. In this case, the transverse components of the magnetic field are written as

$$\mathbf{H}_t^o = \exp\left(i\beta z - i\omega t\right) \sum_{m=-\infty}^{\infty} A_m \left[\left(i\psi_{m+1} - i\psi_{m-1}\right)\mathbf{x} + \left(\psi_{m+1} + \psi_{m-1}\right)\mathbf{y}\right]. \tag{4}$$

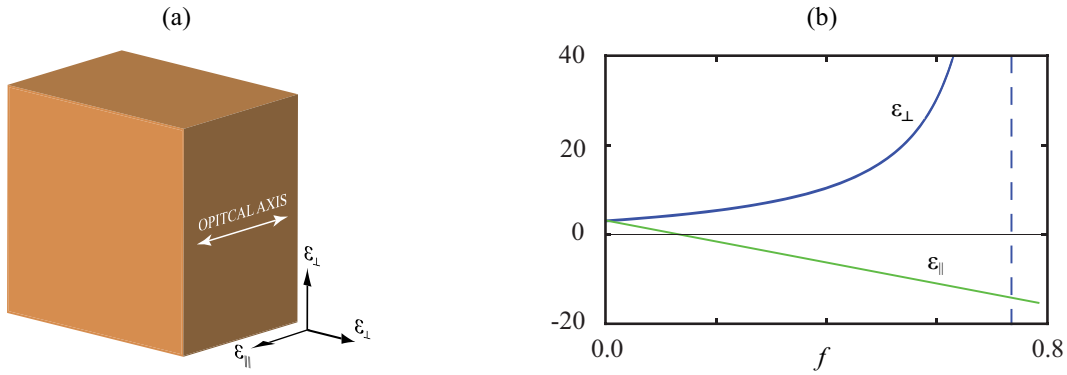

Figure 2. (a) Schematic illustration of the anisotropic medium that substitutes the wire plasmonic crystal of Fig. 1 by using the Maxwell-Garnett model. (b) Variation of $\epsilon_\perp$ and $\epsilon_{||}$ in terms of the filling factor, for silver wires hosted by alumina at $\lambda_0 = 700$ nm.

Let us point out that non-trivial solutions of Maxwell's equations exist involving $H_z^e = 0$. These solutions are associated with extraordinary waves, whose magnetic field may be written as

$$\mathbf{H}_t^e = \exp\left(i\beta z - i\omega t\right) \sum_{m=-\infty}^{\infty} B_m \left[\left(i\psi_{m+1} + i\psi_{m-1}\right)\mathbf{x} + \left(\psi_{m+1} - \psi_{m-1}\right)\mathbf{y}\right], \tag{5}$$

where B_n stands for a complex-valued constant. Now the transverse spatial frequency satisfies $k_t^2 = \epsilon_{||}k_0^2 - \beta^2\epsilon_{||}/\epsilon_\perp$, where[7]

$$\epsilon_{||} = f\epsilon_m + (1-f)\epsilon_d. \tag{6}$$

Some general conclusions may be inferred assuming that $\epsilon_d < |\epsilon_m|$ for visible and infrared frequencies. For numerical purposes we will consider silver and alumina; the permittivities of silver and alumina at the wavelength in vacuum $\lambda_0 = 700$ nm are $\epsilon_{\text{silver}} = -20.4$ (neglecting losses) and $\epsilon_{Al_2O_3} = 3.1$, respectively, taken from experimental data.[8] First of all, note that $0 \leq f \leq f_{\max}$ provided that $a \geq 2r$, where $f_{\max} = \pi/4 \approx 0.78$. On the other hand, $\epsilon_{||} > 0$ for relatively low values of the filling factor,

$$0 \leq f < \frac{\epsilon_d}{\epsilon_d - \epsilon_m}. \tag{7}$$

In the numerical simulation, Eq. (7) yields $0 \leq f < 0.132$. On the contrary, $\epsilon_\perp$ is maintained positive for higher filling factors,

$$0 \leq f < \frac{\epsilon_m + \epsilon_d}{\epsilon_m - \epsilon_d}, \tag{8}$$

which results $0 \leq f < 0.737$ for our metal-dielectric composite. Fig. 2 shows that $\epsilon_\perp$ may take extremely-high positive values in the interval $0.132 \leq f < 0.737$, where $\epsilon_{||}$ is negative. Note that Bessel beams driven by ordinary waves, which are formulated in Eq. (4), cannot exist if $\beta > \sqrt{\epsilon_\perp}k_0$. At the same time, the hyperbolic dispersion of extraordinary waves leads to Bessel beams that may have a propagation constant of ideally any positive value, $0 \leq \beta < \infty$. However, it depends strongly on the sign of $\epsilon_{||}$. For instance, if $\epsilon_{||} > 0$ then $\beta < \sqrt{\epsilon_\perp}k_0$ for the existence of extraordinary waves. On the contrary, solutions involving $\beta > \sqrt{\epsilon_\perp}k_0$ are consistent with EMA provided $\epsilon_{||} < 0$ (and obviously $\epsilon_\perp > 0$). Furthermore, for sufficiently high values of β we find that $k_t \gg k_0$, since $k_t \approx \beta\sqrt{|\epsilon_{||}|/\epsilon_\perp}$. Therefore the spot size of the Bessel beam clearly surpasses the limit imposed by diffraction, leading to subwavelength nondiffracting beams.

In Fig. 3(a) we plot H_x^e taken from Eq. (5) and in Fig. 3(b)-(c) we represent H_x^o from Eq. (4) for Bessel beams propagating with $\beta = 0.8k_0$, that is $\beta = 7.18\ \mu\text{m}^{-1}$. For subfigures (a) and (b) we consider a silver-alumina composite with a filling factor $f = 0.1$; in this case the Maxwell-Garnett model provides the permittivities $\epsilon_\perp = 4.07$ and $\epsilon_{||} = 0.75$. Since both permittivities are positive, dispersion associated with extraordinary waves is ellipsoidal. To evaluate H_x^e we use $B_1 = -i/2 = B_{-1}$, leading to Bessel beams with transverse spatial frequency

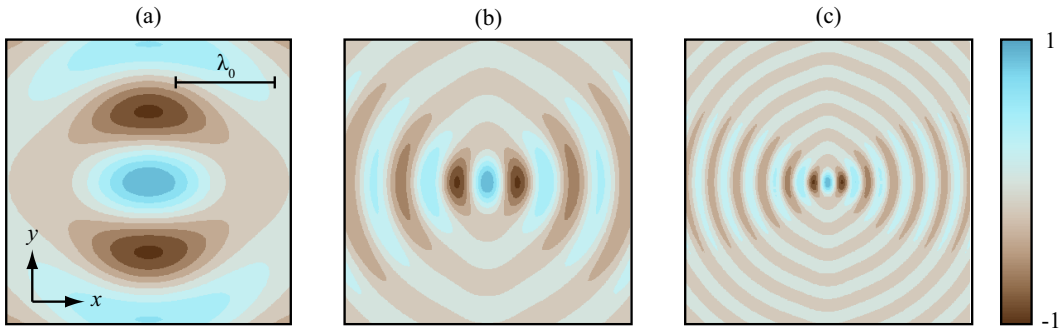

Figure 3. x-component of the magnetic field $\mathbf{H}$ for Bessel beams associated with (a) extraordinary and (b) ordinary waves propagating in a silver-wire medium hosted by alumina ($f = 0.1$) for $\beta = 0.8k_0$. We represent the instantaneous fields H_x^e for $B_1 = -i/2 = B_{-1}$ and H_x^o for $A_1 = i/2 = -A_{-1}$ at $z = 0$ and $t = 0$. In (c) we plot H_x^o for $f = 0.5$. Boxes dimensions of the contour plots are 2 μm $\times$ 2 μm.

$k_t = 7.12$ μm^{-1}. This fact results in a central hot spot whose FWHM is 622 nm along the x axis. On the other hand, the amplitudes $A_1 = i/2 = -A_{-1}$ are set for H_x^o. In this case $k_t = 16.6$ μm^{-1} leading to superresolving hot spots of 146 nm-FWHM on the x direction. However, this effect is slightly weaker along the y axis, as shown in Fig. 3(b). If now we increase the filling factor up to $f = 0.5$, but maintaining the propagation constant β fixed, we observe that no extraordinary waves may be found. It is caused by the negative value of $\epsilon_{||} = -8.67$. In contrast, ordinary waves with extremely-high spatial frequency $k_t = 35.4$ μm^{-1} are obtained in virtue of the giant (and positive) value of $\epsilon_\perp = 16.2$. Fig. 3(c) depicts H_x^o in this case, providing a central peak whose FWHM is 69 nm along the x axis. This fact demonstrates that our Bessel beam clearly features a subwavelength hot spot.

An important characteristic of the Bessel-beam waveforms is in relation with its spatial spectrum. From a mathematical point of view, the transverse spatial spectrum of the wavefield is retrieved by applying the 2D Fourier transform (2D-FT) to its components. By definition, the 2D-FT of a function $g(x, y)$ is derived from $F\{g\}(f_x, f_y) = \iint g(x, y) \exp[-i2\pi(f_x x + f_y y)]dxdy$. By means of the Bessel function closure equation[9] we arrive to the following results

$$F\{\psi_m(r, \phi)\} = 2\pi k_t^{-1}(-i)^m \exp(im\varphi)\delta(k_t - 2\pi\rho), \tag{9}$$

where $(f_x, f_y) = (\rho\cos\varphi, \rho\sin\varphi)$ are set in the polar coordinate system, and δ is the Dirac delta function. If we calculate the 2D-FT to $\mathbf{H}_t^o$ from Eq. (4) and $\mathbf{H}_t^e$ from Eq. (5), separately, we obtain an spatial spectrum consisting of a single ring whose radius is $\rho = k_t/2\pi$. As we will see in the next section, the circular symmetry of the transverse spatial spectrum will lead to an isofrequency curve also with circular symmetry, in contrast to transverse spectra that can be found in arrangements studied elsewhere.[10] Since the value of k_t differs for each polarization, hybrid solutions involving $\mathbf{H}_t^o$ and $\mathbf{H}_t^e$ simultaneously would provide a two-ring shaped spatial spectrum.

3. LOCALIZED FULL-WAVE MODES

Here we compare the above analytical approach obtained from the EMA for the periodic squared array of nanowires with the results of solving numerically the Maxwell's equations. According to the Floquet-Bloch theorem, the magnetic field of a wave mode in a 2D periodic medium with invariant spatial frequency β along the z-axis may be written in the form

$$\mathbf{H} = \mathbf{h}_{\mathbf{k_t}}(x, y) \exp(i\beta z - i\omega t) \exp(ik_x x + ik_y y), \tag{10}$$

where $\mathbf{h}_{\mathbf{k_t}}(x, y)$ is a field with the same periodicity of the medium and $\mathbf{k_t} = (k_x, k_y)$ is the in-plane Bloch k-vector. Nondiffracting beams propagating in wire media may be expressed as a linear combination of the wave modes given in Eq. (10). Therefore we focus on solving the Maxwell's equations to find all $\mathbf{k_t}$ and $\mathbf{h}_{\mathbf{k_t}}$ provided that the propagation constant β is a parameter in our problem. For that purpose we used a commercial finite-element package (COMSOL Multiphysics). In particular, a routine was programmed in the COMSOL RF

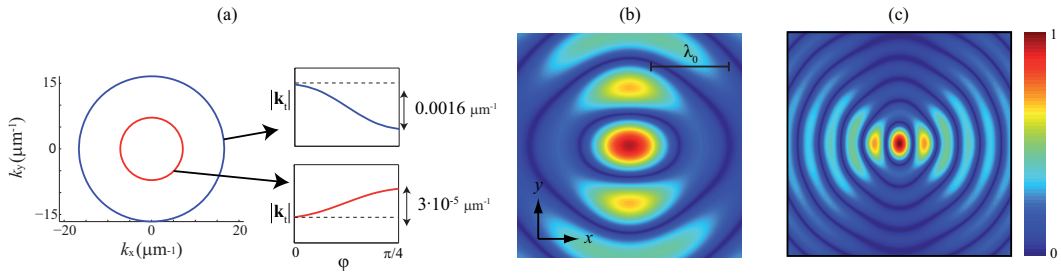

Figure 4. (a) Isofrequency curve for the silver wire medium hosted by alumina ($f = 0.1$) for $\beta = 0.8k_0$. x-component of the magnetic field $\mathbf{H}$ (absolute value) for nondiffracting beams associated with (b) extraordinary waves and (c) ordinary waves. We represent $|H_x|$ that is the result of the Bloch-wave superposition associated with each branch of the spatial spectrum shown in (a).

module that allows to obtain every Bloch mode for a fixed value of β. In other words, we found the complete set of pairs (k_x, k_y), and the corresponding functions $\mathbf{h}_{\mathbf{k_t}}$, which satisfies Maxwell's equations for the prefixed β. This procedure let us to depict the spatial spectrum in the k_xk_y-plane, which is also known as the isofrequency curve, provided a given on-axis frequency β.

In order to verify the validity of our previous analytical results, we start by considering a silver-alumina wired medium with $f = 0.1$ and metallic wires of diameter $2r = 5$ nm. In this case, the lattice period is $a = 14.01$ nm. With these values, $\lambda_0 \gg a$, thus we have a configuration where the EMA is expected to give accurate results. Using our routine based on the finite-element method (FEM) for $\beta = 0.8k_0$ we obtained the isofrequency curve shown in Fig. 4(a). In this case, the isofrequency curve has two branches approaching circles of radius $k_t = 7.16\ \mu\text{m}^{-1}$ and $k_t = 16.6\ \mu\text{m}^{-1}$. The variations of the radius are very small within its corresponding branch. Furthermore, these values of the modulus of $\mathbf{k_t}$ are very near the values of k_t predicted by the EMA for the ordinary wave and the extraordinary wave. In view of these results we previse to obtain nondiffracting beams with waveforms similar to those shown in Fig. 3(a) and (b).

The key point lies on Eq. (9); this equation shows us the way that a complete set of plane waves have to be superposed to generate a Bessel waveform. In the periodic wire medium, Bloch modes will play, in some sense, the role of the plane waves in the anisotropic effective medium. Taking the results shown in Fig. 3(a), we would obtain an equivalent waveform by superposing properly the set of Bloch modes with in-plane k-vectors lying on the quasi-circular branch of radius $k_t = 7.16\ \mu\text{m}^{-1}$. Note that this set contains an infinite number of modes. For numerical purposes, we have selected a finite subset of modes that are evenly spaced in the angular coordinate φ. In the modal superposition, the correct amplitude of each mode can be inferred from the Eqs. (4) and (9). In the case of the extraordinary (ordinary) wave where $B_1 = -i/2 = B_{-1}$ ($A_1 = i/2 = -A_{-1}$), the amplitude is proportional to $1 - \cos 2\varphi$ ($1 + \cos 2\varphi$). Finally, in order to have a localized wave field around a predetermined point (x_0, y_0), which is simply the focus of the nondiffracting beam, we set in-phase the x-component of every function $\mathbf{h}_{\mathbf{k_t}}$ at such point. In our numerical simulations we have set $(x_0, y_0) = (0, 0)$.

In Fig. 4(b) and (c) we plot $|H_x|$ that results from the corresponding superposition of Bloch modes. The aspect of the fields is in a good agreement with that from our analytical approach shown in Fig. 3(a) and (b). From Fig. 4(b) we estimate the FWHM along the x axis as 536 nm that is near 622 nm [from Fig. 3(a)]. Also, the FWHM is 156 nm evaluated from Fig. 4(c), comparable with 146 nm [from Fig. 3(b)].

Finally, we considered an increase of the filling factor up to $f = 0.5$, maintaining the propagation constant $\beta = 0.8k_0$ and the diameter $2r = 5$ nm. Now, the lattice period is $a = 6.27$ nm. From our numerical FEM simulations, shown in Fig. 5(a), we observe that only a single ring of radius $k_t = 37.2\ \mu\text{m}^{-1}$ remains, which is in good agreement with estimations given by the EMA ($k_t = 35.4\ \mu\text{m}^{-1}$). Again the variation of the radius is small, however, it is one order of magnitude greater than that observed for $f = 0.1$. The FWHM of the central hot spot measured along the x-axis is 70 nm [see Fig. 5(b)] that is close to 69 nm measured from Fig. 3(c).

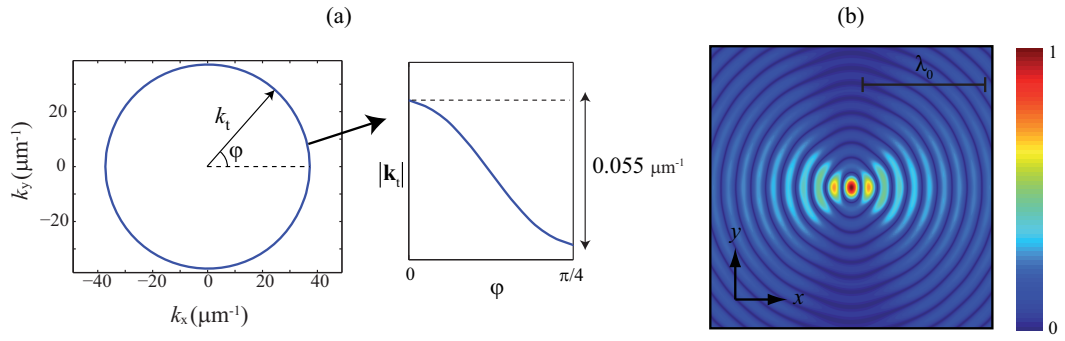

Figure 5. (a) Isofrequency curve for a metallic compound of $f = 0.5$. (b) Wave field $|H_x|$ corresponding to a nondiffracting beam of $\beta = 0.8k_0$ associated with ordinary waves of the effective medium.

4. CONCLUSIONS

We demonstrate the existence of localized nondiffracting beams propagating in a metallic wire medium. The FEM-based numerical simulations are in excellent agreement with the analytical estimations provided by the Maxwell-Garnett model. According to this model, low-filling-factor composites may sustain hybrid Bessel beams having two-ring shaped spatial spectra. On the contrary, high filling factors lead to a single-ring spectrum with a radius that may surpass the limit imposed by diffraction. In particular, we have found that if $\epsilon_{||} < 0$, only one polarization mode associated with either the ordinary wave or extraordinary wave may exist for a given propagation constant β. From physical grounds, this subwavelength effect is attributed to the existing hyperbolic dispersion that is sustained by SPPs in the wires. As a result, subwavelength Bessel beams might be observed experimentally in this sort of periodic composite.

ACKNOWLEDGMENTS

This research was funded by the Spanish Ministry of Economy and Competitiveness under the project TEC2009-11635, and by the Qatar National Research Fund under the project NPRP 09-462-1-074.

REFERENCES

[1] Durnin, J., Miceli, J. J., and Eberly, J. H., "Diffraction-free beams," *Phys. Rev. Lett.* **58**, 1499–1501 (1987).
[2] Manela, O., Segev, M., and Christodoulides, D. N., "Nondiffracting beams in periodic media," *Opt. Lett.* **30**, 2611–2613 (2005).
[3] Miret, J. J. and Zapata-Rodríguez, C. J., "Diffraction-free propagation of subwavelength light beams in layered media," *J. Opt. Soc. Am. B* **27**(7), 1435–1445 (2010).
[4] Miret, J. J., Pastor, D., and Zapata-Rodríguez, C. J., "Subwavelength surface waves with zero diffraction," *J. Nanophoton.* **5**, 051801 (2011).
[5] Zapata-Rodríguez, C. J., Vuković, S., Belić, M. R., Pastor, D., and Miret, J. J., "Nondiffracting Bessel plasmons," *Opt. Express* **19**, 19572–19581 (Sep 2011).
[6] Belov, P. A. and Hao, Y., "Subwavelength imaging at optical frequencies using a transmission device formed by a periodic layered metal-dielectric structure operating in the canalization regime," *Phys. Rev. B* **73**, 113110 (2006).
[7] Sihvola, A., [*Electromagnetic Mixing Formulas and Applications*], Institution of Electrical Engineers, London (1999).
[8] Palik, E. D. and Ghosh, G., [*The electronic handbook of optical constants of solids*], Academic, New York (1999).
[9] Arfken, G. B. and Weber, H. J., [*Mathematical Methods for Physicists*], Academic Press, New York (2001).
[10] Miret, J. J. and Zapata-Rodríguez, C. J., "Diffraction-free beams with elliptic Bessel envelope in periodic media," *J. Opt. Soc. Am. B* **25**, 1–6 (2008).